Gold nanorods as probes in two-photon fluorescence correlation spectroscopy: Emerging applications and potential artifacts

ARTICLE *in* MICROSCOPY RESEARCH AND TECHNIQUE · SEPTEMBER 2013

Impact Factor: 1.15 · DOI: 10.1002/jemt.22242 · Source: PubMed

4 AUTHORS, INCLUDING:

Wei Shih-Chung

National Taiwan University

14 PUBLICATIONS **133** CITATIONS

SEE PROFILE

Chii-Wann Lin

National Taiwan University

224 PUBLICATIONS **1,771** CITATIONS

SEE PROFILE

Gold Nanorods as Probes in Two-Photon Fluorescence Correlation Spectroscopy: Emerging Applications and Potential Artifacts

DA-SHIN WANG,[1] SHIH-CHUNG WEI,[2] SHIH-CHU LIAO,[3] AND CHII-WANN LIN[1,2]*
[1]*Institute of Biomedical Engineering, College of Medicine and Engineering, National Taiwan University, Taipei, Taiwan*
[2]*Institute of Biomedical Electronics and Bioinformatics, College of Electrical Engineering and Computer Science, National Taiwan University, Taipei, Taiwan*
[3]*ISS, Inc, Champaign, Illinois 61822*

KEY WORDS gold nanorods; fluorescence correlation spectroscopy; excitation saturation; rotational diffusion; photothermal effects

ABSTRACT Owing to the highly efficient two-photon fluorescence of gold nanorods and very short fluorescence lifetime compared with the rotational correlation time, the rotation and diffusion of a single gold nanorod can be easily observed by two-photon fluorescence correlation spectroscopy (TP-FCS). This property, along with the previous successful use as a contrast agent in two-photon fluorescence imaging, suggests a potential application in TP-FCS as well. Although the FCS measurement becomes highly efficient with gold nanorods as probes, the amplitude and temporal decay of the measured correlation functions depend critically on excitation power. Here, we investigate various photophysical processes of gold nanorods to determine the cause of such a sensitive power dependency. This understanding provides a basis for choosing appropriate FCS models to recover reasonable physical parameters. Although the correlation function amplitude $G(0)$ is 32 times lower when the excitation power increases from 20 μW to 1.12 mW, the application of a saturation-modified FCS model yields very good fit to each data set and the fitted concentration of 0.64 nM is comparable to the 0.7 nM given by the inductively coupled plasma mass spectrometry measurement. The FCS assay appears to be an efficient method for the quantification of gold nanorods when correctly interpreted. However, even with the saturation considered in the fitting model, the fitted rotational and translational diffusion rates are getting faster as the power increases. This indicates that other effects such as photothermal effects may raise the local temperature, and thus increasing the rotational and translational diffusion rate. *Microsc. Res. Tech. 76:882-889, 2013*.

INTRODUCTION

Fluorescence correlation spectroscopy (FCS) is a technique that measures the time-dependent fluctuation of a system-emitting fluorescence or any other forms of luminescence. The measurement of fluctuation is a relatively accurate process, as opposed to the measurement of absolute emission intensity, which usually carries substantial uncertainty and requires a reference standard for analysis. FCS records the autocorrelation function of spontaneous fluctuations in a system at its thermal equilibrium, and in principle, all physical parameters that give rise to characteristic fluctuations are accessible by FCS (Magde et al., 1972; Schwille and Haustein, 2009; Thompson, 1991). It is particularly useful for the in situ measurement of molecular concentration and mobility. The major difficulty encountered in the early development of FCS is a poor signal-to-noise ratio (S/N). The basic problem is that fluctuation manifests prominently only in a system of small numbers. To make the fluctuation large enough to yield a good S/N and thus become experimentally observable, only a few molecules are allowed to be detected. This explains the reason why FCS is generally more sensitive to extremely low concentrations of analytes from nanomolar down to a single-molecule level. The improvement of FCS sensitivity to submicromolar analytes relies on a smaller detection volume, which is made possible by confocal detection and two-photon excitation. Typically, the detection volume can be limited to <1 fL in these cases (Berland et al., 1995). The two-photon excitation has the special advantages of penetrating deep into tissue and thus provides a way to arbitrarily sample the fluctuation of a region of interest in a three-dimensional sample (Larson et al., 2003). Although other ultrasensitive analysis techniques, such as inductively coupled plasma mass spectrometry (ICP-MS), offer high sensitivity down to 0.01 ppb, FCS provides unparalleled advantages to measure not only the concentration but

Additional Supporting Information may be found in the online version of this article.

*Correspondence to: Chii-Wann Lin, Institute of Biomedical Engineering, National Taiwan University, No. 1, Sec. 4 Roosevelt Rd., Taipei, Taiwan. E-mail: cwlinx@ntu.edu.tw

Received 22 April 2013; accepted in revised form 19 May 2013

Contract grant sponsor: National Science Council of Taiwan (NSC); Contract grant number: 099-2811-E-002-127.

DOI 10.1002/jemt.22242
Published online 8 June 2013 in Wiley Online Library (wileyonlinelibrary.com).

also the mobility of fluorescence-tagged molecules in intact living tissues, opening an avenue to the in situ and in vivo biochemistry of living samples (Bacia and Schwille, 2003; Pitschke et al., 1998).

The FCS measurement benefits greatly from a bright fluorescent probe, which helps to reduce the interference from background noise; it is particularly true for biological specimen as the inherent autofluorescence is often strong. For probes with lower fluorescence efficiency, a longer measurement time is usually required to improve the *S/N*, resulting in a lower temporal resolution. The gold nanorod has been demonstrated to emit strong two-photon fluorescence (TPF) owing to the enhancement of absorption through the longitudinal surface plasmon (LSP) modes (Wang et al., 2005, 2009). The gold nanorod has been widely utilized as a luminescent probe in TPF imaging and also as a hyperthermic target (Fu et al., 2010; Huff et al., 2007). For the same reason, the gold nanorod can be a potential two-photon FCS (TP-FCS) probe to detect the analyte of ultralow concentrations. It has a significant advantage over many fluorescent dyes because most dyes, at very long concentration (<1 nM), do not produce photon counts large enough to yield a satisfactory autocorrelation curve within a short time (seconds), which greatly hinders the application of FCS to low concentration analytes. Furthermore, the TPF of gold nanorods emerges only when the long axis of the rod is aligned with the polarization of the excitation light (Bouhelier et al., 2005; Wang et al., 2005), and hence the rotational motion may be detected with simple TP-FCS technique. Theoretically, rotational diffusion is more sensitive to size than translational diffusion, making rotational diffusion a better method to monitor the binding of molecules (Tsay et al., 2006). Fluorescent dye molecules also have this property; however, the rotation of fluorescent molecules occurs on a similar time scale as other processes, such as fluorescence lifetime and triplet blinking, thus becomes difficult to differentiate (Schwille and Haustein, 2009). In the case of nanorods, the rotation is well separated from its fluorescence lifetime with the rotational motion occurring on the microsecond (μs) range and fluorescence lifetime of <100 picoseconds (ps) (Zhang et al., 2010). Not only are gold nanorods potential probes for TP-FCS, but TP-FCS is also a useful tool for the quantification of gold nanorods. Gold nanorods are generally synthesized with concomitant gold nanospheres. Quantification of the gold nanorod concentration requires further purification of the particles (Sharma et al., 2009). As TPF efficiency is shape-selective, in which only nanorods with a specific aspect ratio carry the SP mode to strongly absorb the excitation light, TP-FCS is possible to selectively measure the concentration of nanoparticles with certain shapes in a mixed solution.

In this study, we use TP-FCS to measure the concentration and diffusion coefficient of colloidal gold nanorods and investigate the accuracy by comparing the results of TP-FCS and of ICP-MS, which is currently considered as the standard method for the quantification of metallic nanoparticles. The measurement is very efficient; without the need to predigest nanorods, TP-FCS can acquire results in seconds, much faster than the ICP-MS measurement. Although it is a highly sensitive, fast, and convenient method, measuring gold nanorods with FCS is not as straightforward as the case of fluorescent dyes. Generally, high excitation power is preferred in FCS measurement to optimize the fluorescence signal; however, the measured autocorrelation function of colloidal gold nanorods is considerably intensity-dependent. The result raises further consideration as to whether the measurement itself perturbs the system with some intensity-dependent effects such as optical trapping (Ehrenberg and Rigler, 1974) and laser photothermal melting (Link et al., 1999), or the observation conditions have been altered by intensity-related artifacts such as excitation saturation (Berland and Shen, 2003). This understanding helps us to select an appropriate model to interpret the autocorrelation function, which can then return accurate physical parameters. It also helps the user to identify the optimized experimental conditions and avoid possible artifacts in using gold nanorods as FCS probes.

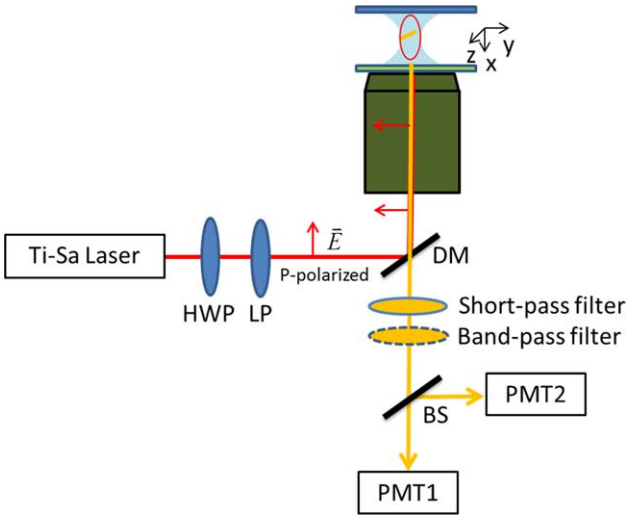

Fig. 1. Schematic diagram of the experimental setup. HWP, half-wave plate; LP, linear polarizer; DM, dichroic mirror; BS, beam splitter; PMT, photomultiplier tube. [Color figure can be viewed in the online issue, which is available at wileyonlinelibrary.com.]

MATERIALS AND METHODS

Colloidal Gold Nanorod

The gold nanorod solution is purchased from Nanopartz. The axial size and length of the gold nanorods are labeled by the manufacturer as 10 and 35 nm, respectively. The corresponding LSP mode is at 753 nm. The quantification of gold content is performed on an ICP-MS (7500CE, Agilent) by further diluting the nanorod solution. The gold quantity in the nanorod solution is calibrated as 22.03 ppm, which is equivalent to a 0.7-nM particle concentration.

FCS Setup

The experimental setup for the FCS measurement is shown schematically in Figure 1. The setup is constructed on an inverted microscope (IX70, Olympus) with a 60× objective lens (Olympus UPLSAPO NA = 1.2). The light source is a pulsed Ti:sapphire laser (Tsunami, Spectra-Physics) operating at 780 nm

with a pulse width of <100 fs and a repetition rate of 80 MHz. A half-wave plate (HWP) is inserted between the laser and a linear polarizer (LP) to adjust the intensity of the laser while keeping the polarization fixed at a certain orientation. A dichroic mirror is set in a cube to separate the excitation and emission light. A short-pass filter and a band-pass filter (660 ± 25 nm) are placed in the detection path to eliminate the laser backscattering and selectively capture the fluorescence emission from gold nanorods. The FCS is obtained by sending the detected photon pulses to a hardware correlator card (3XDAC and FCS card, ISS). For the detection of the rotation, the sampling frequency is set at 1 MHz in our experiment, and the sampling time is 50 s. To eliminate possible correlation signals generated by detector afterpulsing, a beam spliter is inserted in front of two detectors and the crosscorrelation is then acquired as a checking reference.

RESULTS

Excitation Power-Dependent Autocorrelation Function

The fluorescence autocorrelation function $G(\tau)$ is defined as $G(\tau) \equiv \langle F(t)F(t+\tau)\rangle = \int_0^\infty F(t)\cdot F(t+\tau)\mathrm{d}t$, which evaluates the autocorrelation of the fluorescence intensity function $F(t)$ after a time lag τ. For fluorescent particles freely diffusing in and out of the excitation volume, the $G(\tau)$ can be modeled using simple Brownian diffusion with an estimation for the detection volume. The profile of the two-photon detection volume is best approximated as a Gaussian–Lorentzian (GL) squared (Berland et al., 1995); but for FCS purposes, it can be simplified by taking the square of the focal volume, which is a 3D Gaussian by first approximation (Schwille and Haustein, 2009). Therefore, for particles undergoing Brownian diffusion in the detection volume, the $G(\tau)$ measured by TP-FCS can be expressed as (Barcellona et al., 2004; Thompson, 1991)

$$G(\tau) = \frac{\gamma_{3DG}}{C V_{3DG}} \frac{1}{\left(1+8D\tau/\omega_0^2\right)} \frac{1}{\left(1+8D\tau/z_0^2\right)^{\frac{1}{2}}}, \qquad (1)$$

where C is the local particle concentration, is the geometric prefactor for 3D Gaussian model, which is about 1/22, $V_{3DG} = (\pi/4)^{3/2}\omega_0^2 z_0$ represents the effective detection volume, D is the diffusion coefficient, and ω_0 and z_0 are the beam waist in the radial and axial directions, respectively. Compared with the $G(\tau)$ of 1 nM 0.1-μm beads, the $G(\tau)$ of the gold nanorods exhibits two characteristic decay times as shown in Figure 2. These two characteristic decays consistently appear in all measured $G(\tau)$ of the gold nanorods. The common decay time on the millisecond scale is attributed to the Brownian translational diffusion, and the very short decay time on the microsecond scale is identified as the rotational diffusion of gold nanorods. The TPF of gold nanorods is bright owing to enhanced absorption by the LSP mode (Wang et al., 2009), and the strength of the absorption depends on $|\vec{\mu}_{SPR}\bullet\vec{E}|^4$, which is proportional to $\cos^4\theta$, where $\vec{\mu}_{SPR}$ is the LSP dipole, $\vec{E}$ is the electrical field, and θ is the angle in between. Only the rods with their long axis aligned to the laser polarization emit strong fluorescence. Moreover, the fluorescence lifetime of gold nanorods is found to be <100 ps (Zhang et al., 2010), much shorter than the rotational diffusion time. We also measured the fluorescence lifetime of colloidal gold nanorods by frequency-based technique and it was found to be 80 ps (Supporting Information Fig. S1). As the TPF of gold nanorods emits in a relatively short lifetime and the intensity fluctuates with the angle θ, the FCS measurement performed with linearly polarized light is a good technique to probe the nanorod's rotation (Fig. 1). The fourth power dependence on $\cos\theta$ also indicates that TPF is more sensitive to the rotational motion than the one-photon method.

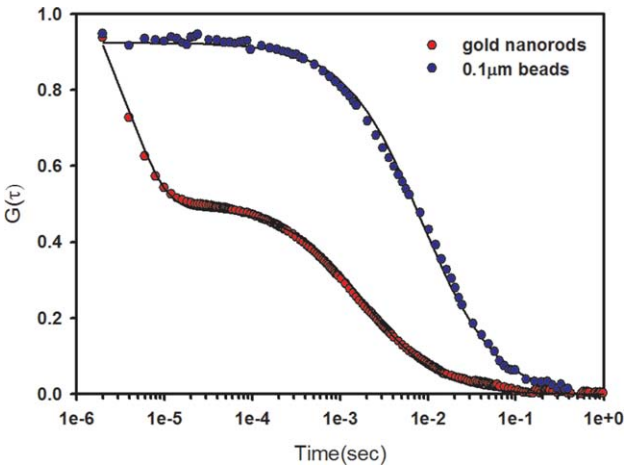

Fig. 2. FCS curves of colloidal gold nanorods (red circles) and 0.1-μm fluorescent beads (blue circles) sampled at 500 kHz. The circles are experimental data; solid lines represent good fits to the data using 3D Gaussian model. [Color figure can be viewed in the online issue, which is available at wileyonlinelibrary.com.]

To interpret the $G(\tau)$ of gold nanorods with an appropriate model, the rotational diffusion component needs to be incorporated into $G(\tau)$. If the rotational and translational diffusions are independent, the total correlation function, $G(\tau)$, can be separated as two terms:

$$G(\tau) = G_R(\tau)\times G_D(\tau) \qquad (2)$$

The term G_D takes the same form as Eq. (1). The expression for $G_R(\tau)$ is, however, complex and depends on many factors, such as the laser polarization and the observation with or without the polarizer. In the simplest case, when the excitation light is linearly polarized and all emitted photons are collected with equal probability, the rotational correlation function can be expressed as (Barcellona et al., 2004; Ehrenberg and Rigler, 1974)

$$G_R(\tau) = 1 + R\exp\left(-\tau/\tau_R\right) \qquad (3)$$

where R depends on the degree of polarization of the fluorophore (Tsay et al., 2006), and τ_R is the rotational correlation time. Equation (2) is used to fit the measured $G(\tau)$ to acquire the concentration and diffusion coefficient of colloidal gold nanorods. Computing the concentration and diffusion coefficient of the gold nanorods from FCS measurement appears to be

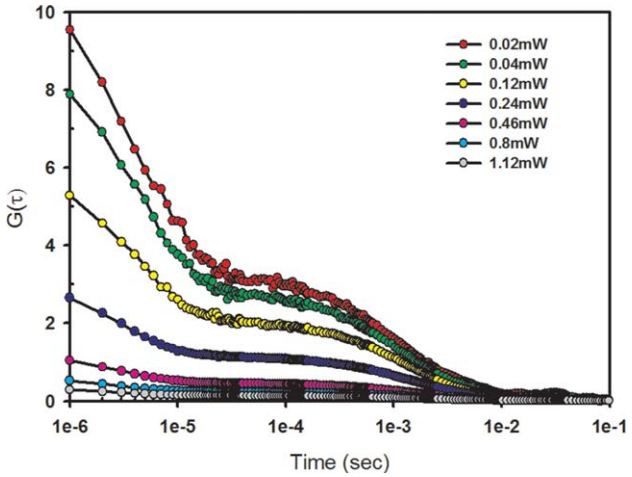

Fig. 3. The intensity-dependent FCS curves of gold nanorods. [Color figure can be viewed in the online issue, which is available at wileyonlinelibrary.com.]

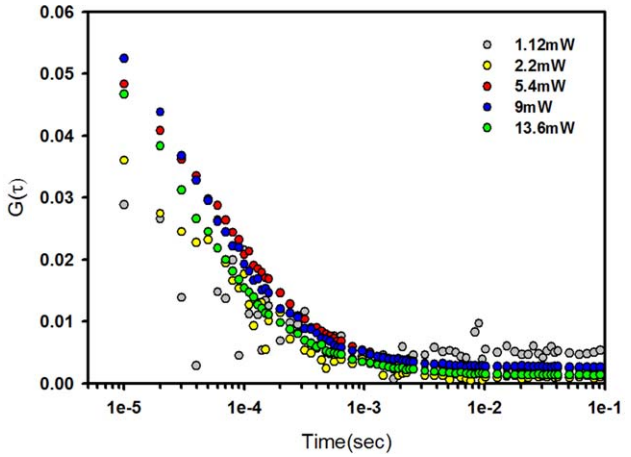

Fig. 4. Intensity-dependent FCS curves of 20 nM Rhodamine 6G dye; the gray circles show a less accurate FCS curve at lower excitation power. [Color figure can be viewed in the online issue, which is available at wileyonlinelibrary.com.]

straightforward with the well-built model described in Eq. (2). However, $G(\tau)$ of the gold nanorods is considerably excitation power-dependent as shown in Figure 3. For example, $G(\tau)$ is extremely flattened at higher powers (>1 mW). The power dependence makes the quantification of colloidal gold nanorods by FCS a little bit confusing. The correlation function amplitude $G(0)$ is 32 times lower when the excitation power increases from 20 μW to 1.12 mW. The low $G(0)$ generally represents an increase of particles in the detection volume, thus making the correlation very low. The increase of particles can be attributed to two reasons: first, the excitation saturation modifies the size and shape of the detection volume and thus more particles are detected (Berland and Shen, 2003); second, the laser can trap particles in the focus, a process that depends dramatically on the applied power (Pelton et al., 2006). In the first case, more particles are detected while the concentration remains constant, which requires a model characterizing the volume change; however, in the second case, the measurement has become invalid as excitation laser traps particles in the focus and changes the local concentration.

Saturation Effects Versus Optical Trapping

The mechanism of fluorescence saturation is well known as a depletion of the ground state population, in which higher excitation levels no longer increase the excitation rate and hence the fluorescence emission rate reaches its maximum. The onset of excitation saturation occurs first from the center of laser focal volume and expands outward as the excitation power increases; therefore the excitation profile varies at different excitation levels (Berland and Shen, 2003). It is understood the excitation saturation will influence FCS measurement; however, it is not generally considered in regular FCS practices. In regular FCS practice, a standard fluorescent dye or bead solution is used to calibrate the beam waist ω_0 and z_0 and the calibrated beam waist is subsequently used as a fixed parameter in the model fitting. Generally, $G(\tau)$ of a typical fluorescent dye is approximately the same over a wide range of two-photon excitation power. For example, $G(\tau)$ of 20 nM Rhodamine dye acquired in our TP-FCS system does not exhibit distinctive difference in an excitation power ranging from 1.12 to 13.6 mW, an 11-time increase in power (Fig. 4). The explanation is that typical dye molecules do not reach saturation in normal power range of TP excitation owing to a low two-photon absorption cross-section. The profile of observation volume remains roughly the same in a wide power range, and hence the calibrated beam waist at a specific excitation power and the typical 3D Gaussian model are generally applicable. As gold nanorods have a high two-photon absorption cross-section owing to surface plasmon resonance, saturation can begin at very low excitation power and slight increase in excitation power after that can have dramatic effects in the size of observation volume.

Besides excitation saturation, the laser can trap gold nanorods in the focus (Jones et al., 2009; Pelton et al., 2006; Tong et al., 2009; Toussaint et al., 2007). Optical trapping is to be avoided as it alters the physical parameters of interest by enhancing the local concentration and slowing down the diffusion rate. Either of these two mechanisms, optical trapping and excitation saturation, or a combination of both, can be postulated to explain the lower $G(0)$ and slower temporal decay at higher excitation power. It is necessary in our study to evaluate the significance of these two effects and differentiate one from the other.

Optical trapping of a nanosized particle has been a challenging task because the scattering force outweighs the gradient force as the size shrinks, which tends to push particles along the beam's propagation direction (Toussaint et al., 2007). Stable optical trapping of gold nanoparticles has been accomplished by exploiting the surface plasmon resonance. It was mainly carried out with a CW laser at a near resonance condition, slightly red-shifted from the LSP resonance wavelength (Pelton et al., 2006; Toussaint et al., 2007). The power used for trapping was reported from 15 to 60 mW delivered on the sample (Jones et al., 2009; Pelton et al., 2006; Tong et al., 2009;

TABLE 1. The fit results of colloidal gold nanorod at various excitation powers using a 3D Gaussian model (Eq. (2))

Power on sample (mW)	Concentration (nM)	Translational diffusion coefficient ($\mu m^2/s$)	Rotational correlation time (μs)	Fitting mean square error
0.02	0.75	12.64	5.67	0.44
0.04	0.87	12.41	5.32	0.42
0.12	1.16	12.27	4.67	0.71
0.24	2.12	9.79	3.69	0.61
0.46	5.29	9.36	3.63	0.42
0.8	10.48	7.86	3.63	0.26
1.12	17.88	6.57	3.77	0.62

TABLE 2. The fit results of colloidal gold nanorod at various excitation power using a saturation-modified FCS model

Power on sample (mW)	Concentration (nM)	Translational diffusion coefficient ($\mu m^2/s$)	Rotational correlation time (μs)	ω_0 (μm)	I_{sat} (mW)	Fitting mean square error
0.02	0.64	12.04	5.66	0.31	0.040	0.42
0.04	0.64	12.78	5.32	0.31	0.047	0.34
0.12	0.64	14.41	4.68	0.31	0.076	0.36
0.24	0.64	19.27	3.70	0.31	0.082	0.52
0.46	0.64	29.14	3.60	0.31	0.088	0.66
0.8	0.64	30.44	3.57	0.31	0.115	0.28
1.12	0.64	29.33	3.70	0.31	0.136	0.37

Toussaint et al., 2007). One characteristic for the stable trapping is the alignment of nanorod's long axis with the laser polarization, which means that the rotational motion is suppressed (Pelton et al., 2006). However, we have consistently measured the rotational signals of gold nanorods from FCS even at a relatively high power (30 mW delivered on the sample). Another reason we dismiss the possibility of optical trapping is the absence of an increasing brightness from the focal point emission as a result of consecutive trapping (Deng et al., 2012; Toussaint et al., 2007). An important factor distinguishes our experiment from the previous studies is that we used a femtosecond-pulsed Ti:Sapphire laser, whereas previous studies (Jones et al., 2009; Pelton et al., 2006; Tong et al., 2009; Toussaint et al., 2007) utilized a continuous-wave (cw) laser for trapping. Though a recent study has suggested that the femtosecond laser is as effective as cw systems for trapping dielectric spherical particles in the Rayleigh and Mie regimes (Agate et al., 2004; Malmqvist and Hertz, 1995), its capability of trapping gold nanorods is still very limited (Deng et al., 2012) possibly owing to the higher-order nonlinear effects. Even if the nanoparticles are trapped by a pulsed laser, it generally requires higher energy and occurs in a different manner. Jiang et al. have reported a completely new trapping phenomenon that relates to the nonlinear effects, in which gold nanoparticles are trapped in two stable sites by a femtosecond laser with a threshold power as high as 80 mW (after passing through the objective lens) (Jiang et al., 2010). Therefore, it is unlikely that optical trapping occurs in our system and causes such a large variation of $G(\tau)$ as shown in Figure 3.

It then implies that excitation saturation is the major cause for the variation of $G(\tau)$ as shown in Figure 3. It is noted that although $G(\tau)$ is highly influenced by the excitation saturation, in most cases it can be well fitted using the unsaturated 3D Gaussian model. However, such fits often yield unreasonable results (Nagy et al., 2005). For example, $G(\tau)$ in Figure 3 can be fit quite well with the 3D Gaussian model in which the beam waist ω_0 and z_0 is set fixed as 0.3 and 1.2 μm, respectively. The result is smmarized in Table 1. The results give us a completely different physical picture. It suggests an increasing local concentration and a slowing down of diffusion as the excitation power goes up, which would easily lead to the conclusion of optical trapping in this system. Nagy et al. have proposed a FCS fitting model to include the saturation effects; the model exploits the mathematical simplicity of the 3D Gaussian model while also incorporating the saturation effects on the detection volume (Nagy et al., 2005). The approach is to introduce three scaling factors for the ratio γ/V and beam waist (ω_0 and z_0) in the 3D Gaussian model. The scaling factors depend only on the saturation parameter, $R_{sat} = I_0/I_{sat}$, which specifies the excitation intensity relative to the saturation intensity. The saturation-modified model for FCS fitting can be written in the following form

$$G_D(\tau) = \frac{1}{C}\frac{\chi_{\gamma/V}\times\gamma_{GL}}{V_{GL}}\frac{1}{\left(1+8D\tau/\chi_\omega\omega_0^2\right)}\frac{1}{\left(1+8D\tau/\chi_z z_0^2\right)^{1/2}} \quad (4)$$

where $\chi_{\gamma/V}$, χ_ω, and χ_z represent the scaling factors for γ/V, ω_0, and z_0, respectively. It is noted that the GL profile is used in this formalism because it provides a more accurate representation of two-photon excitation profile and is superior for describing the observed saturation-induced variations in volume (Nagy et al., 2005). The unsaturated volume for the GL distribution is $V_{GL} = \pi^3\omega_0^4/4\lambda$, with a gamma factor $\gamma_{GL} = 3/16$, and z_0 by GL model is approximately $3.2\pi\omega_0^2/\lambda$. The scaling factors are not fitting parameters; they depend explicitly on R_{sat} and the scaling factors as functions of R_{sat} are first derived by computing the observation volumes and beam waist at different excitation levels (Nagy et al., 2005).

We employ the saturation-modified FCS model described above to interpret our data. The measured $G(\tau)$ in Figure 3 was thus fit with Eq. (4) multiplied by the rotational term $G_R(\tau)$ in Eq. (3). The beam waist (ω_0) and local concentration (C) are set as global fitting parameters for the $G(\tau)$ data series. However, because the plasmon-enhanced absorption rate critically depends on the shape of gold nanorod, the saturation intensity can vary if gold nanorods are melted and deformed at higher excitation power. Unlike the fitting for fluorescent molecules, which generally have constant absorption rate and hence the saturation intensity (I_{sat}) is set as a constant (global) fitting parameters across all $G(\tau)$ data sets, here I_{sat} is fit individually for each excitation level. Hence, each $G(\tau)$ data set is fit to acquire its unique values for saturation intensity (I_{sat}), translational diffusion coefficient (D), and rotational correlation time (τ_R). The results are summarized in Table 2. The saturation-modified model in Eq. (4) fits all $G(\tau)$ quite successfully. The goodness of each curve fitting is shown in Supporting

Information Figure S2. The recovered beam waist and concentration are 0.31 μm and 0.64 nM, respectively. With the modified model to account for the saturation induced volume changes, we are able to find a constant concentration which can fit well to all $G(\tau)$. The fit concentration is 0.64 nM, very close to the measured result by ICP-MS, which yields an estimation of 22.02 ppM, corresponding to a 0.7-nM particle concentration for the 10×35 nm gold nanorod.

Unlike ICP-MS which needs to predigest the gold nanorods in solvent, TP-FCS is a fast, nondestructive, and in situ technique to measure the concentration of gold nanorods. However, the measurement can easily get saturated as the I_{sat} can be as low as 40 μW, 170 times lower than a Rhodamine 6G dye (Nagy et al., 2005). Avoiding the saturation issues is not easily achievable by simply working with the excitation powers for which the total measured fluorescence maintains its quadratic dependence on excitation intensity. Observing only the quadratic dependence of fluorescence intensity has been proved to underestimate the importance of saturation (Wu and Berland, 2007). It is especially true for gold nanorods because the I_{sat} may be modified by possible shape changes owing to photothermal effects. Applying a saturation-modified model in this case is helpful in determining I_{sat} and local concentration from TP-FCS measurement.

DISCUSSION

If we normalize all $G(\tau)$ in Figure 3, the $G(\tau)$ measured at higher power generally exhibits a longer millisecond temporal decay, which will yield a slower diffusion coefficient if fitted by a typical 3D Gaussian model (Table 1). It can be easily understood within the context of excitation saturation because it takes a longer time for the particle to escape from the enlarged detection volume. One thing we expect from the saturation-modified FCS model is that the recovered diffusion coefficients will be roughly the same at different excitation powers as mentioned in the previously published reports (Nagy et al., 2005), which it clearly is not (Table 2). Over a time equal to the rotational correlation time, the gold nanorods transition from early time anisotropic motion to an isotropic diffusion, which can be well described by a single average diffusion coefficient. The theoretical diffusion coefficient of a 10×35nm gold nanorod is 14.1 $\mu m^2/s$ (Han et al., 2006). To our surprise, the diffusion coefficient increases substantially when the power is 0.24 mW or above. A common reason for the increase in diffusion coefficient from FCS fitting is photobleaching of the fluorescent dye, in which a dye is photochemically destroyed and thus disappears before actually leaving the detection volume. This leads to a faster decay of fluorescence signal which then results in a faster diffusion coefficient in fitting. Although gold nanorods are not susceptible to photobleaching, they go through shape transformation upon the exposure to low-energy femtosecond laser pulses (Link et al., 1999, 2000a,b). Though the heat generated by femtosecond laser pulse melts nanorods, the shape changes do not in principle change the diffusion rate of the nanorods; the diffusion coefficients of the rods melted into various aspect ratios are around the same as shown in Supporting

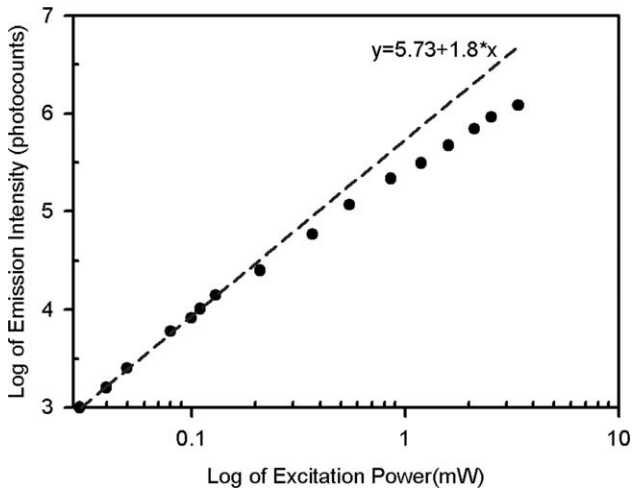

Fig. 5. Emission intensity dependence of gold nanorods on excitation power at 780 nm as measured from the setup in Figure 1.

Information Figure S3. However, as the fluorescence is reduced by the shape deformation, the effect induced by photothermal melting is very similar to that caused by photobleaching. Photobleaching models for FCS have been developed previously (Widengren and Rigler, 1996) in which the $G(\tau)$ is multiplied by a series of exponential terms $\left[1+\sum_i B_i[\exp(-k_{Di}\tau)-1]\right]$. B_i denotes the bleaching fraction because some dye molecules remain intact after passing through the detection volume. There can be different photodestruction pathways, and hence multiple photobleaching factors ($i > 1$) are introduced into the model. This model has been used to account for the photobleaching of fluorescent dyes in FCS measurement and recover correct diffusion coefficients. Generally, a monoexponential ($i = 1$) bleaching factor is generally sufficient for the fitting (Berland and Shen, 2003; Nagy et al., 2005; Widengren and Rigler, 1996); however, we are unable to obtain satisfactory fitting even employing two photobleaching factors ($i = 2$). The photobleaching effects alone do not fully explain our observation. Gold nanorods under strong illumination indeed are subjected to photothermal melting and followed by a reduction in fluorescence emission, but the previous study indicates that for gold nanorods randomly diffusing in water and illuminated with tens of milliwatt focal power, the rod is slightly reduced in aspect ratio rather than transformed all the way into spheres (Pelton et al., 2006). It is also clear from Figure 5 that though the fluorescence emission starts to deviate from the quadratic dependence on excitation power at ~0.13 mW, which seems to indicate photobleaching caused by photothermal melting, the emission is still very bright, showing gold nanorods remain elongated rather become spheres as spheres have almost no TPF (Wang et al., 2009). The brightness of fluorescence is slightly diminished instead of completely destructed, and hence the photobleaching model for fluorescent molecules is not easily applicable. Moreover, the optical absorption from gold nanorods also heats the surrounding water and generates "hot Brownian motion." The temperature and viscosity "felt" by the heated nanoparticle are

not simply the surface conditions and need to be calculated over the whole solvent (Rings et al., 2010). According to the theoretical calculations (Rings et al., 2010), a hot Brownian particle performs a random diffusion characterized by an effective diffusion coefficient which increases nonlinearly with the local temperature. The increased diffusion rate in Table 2 may not simply be an artifact but can be the manifestation of the hot Brownian motion.

Another evidence for the hot Brownian motion is the increased rate of rotational diffusion. It has been proposed previously that the rotational diffusion coefficient (D_R) of nanorods appears to be a better observable because it is more sensitive to size changes and is not affected by the size of observation volume as the translational diffusion coefficient is (Tsay et al., 2006). Its value remains the same regardless of chosen models for $G_D(\tau)$ (Tables 1 and 2). While this idea is true, the rotational diffusion coefficient can be affected by excitation saturation. The excitation saturation also makes it less sensitive to detect the rotational motion through fluorescence fluctuation. As the power increases to the saturation level, drop in fluorescence is not clearly seen until the long axis of nanorod is perpendicular to the laser polarization; hence, the rotational correlation time (τ_R) is expected to be longer if saturation effects dominate in the process. However, a decreased τ_R, which corresponds to an increased rotational diffusion rate, is observed in Tables 1 and 2. The simultaneous increases in both translational and rotational diffusion rates are strong evidences for the heated nanorods undergoing hot Brownian motion.

Our results indicate that, although gold nanorods are very efficient fluorescent probes, the FCS measurement using gold nanorods as probes should be limited to the low excitation power regime (<40 μW) to avoid the artifacts resulting from excitation saturation and photothermal heating. Otherwise, the saturation-modified model should be employed for an accurate estimation of local concentration. According to the previous study (Nagy et al., 2005), the saturation-modified excitation profile is related only to saturation parameter ($R_{sat} = I_0/I_{sat}$). Therefore, although the saturation issue affects most fluorescent dye molecules, the $G(\tau)$ of gold nanorods is much more sensitive to the excitation power as the I_{sat} for gold nanorod is much lower than that of a fluorescent molecule, which is about several milliwatts. In this regards, gold nanorods and typical fluorescent molecules are simply two kinds of FCS probes working at different power ranges; the former requires very fine adjustment in microwatts range, whereas the latter has relatively large working power range. This seems to suggest that gold nanorods do not provide special benefits as FCS probes; however, simply reducing the excitation power to microwatts level is an advantage as it poses less photodamage to the sample and demands less on the FCS system. Keeping the gold nanorod working at an unsaturated (~20 μW) level already provides signals good enough to detect subnanomolar analytes in seconds as shown in Figure 3; on the other hand, it is still very difficult to detect subnanmolar Rhodamine dye even with the highest power of our system (~30 mW). To avoid optical saturation and eliminate photodamage while simultaneously achieving satisfactory *S/N* in TP-FCS, gold nanorod appears to be a better choice over a typical fluorescent molecule.

CONCLUSIONS

We have demonstrated the use of gold nanorods as FCS probes and made it possible to resolve both translational and rotational diffusion and rotation. The measured autocorrelation function is highly dependent on excitation power in which lower $G(0)$ and slower temporal decay are observed at higher excitation power. A further investigation to clarify the effects of excitation saturation, optical trapping, and photothermal melting on $G(\tau)$ is carried out. Based on the results described in previous passages, it can be concluded that:

1. Optical excitation saturation plays an important role in the low $G(0)$ observed at high power and is the major cause for an overestimation of local concentration. With the application of a saturation-modified FCS model, a more accurate estimation of local concentration is achieved, which is comparable to the results from ICP-MS.
2. Even with the application of a saturation-modified TP-FCS model, it does not successfully yield a constant diffusion coefficient comparable to the theoretical one. The diffusion coefficient increases substantially as power gets larger than 0.24 mW. A general model of fluorescence bleaching cannot account for the increasing diffusion rate at higher power. It is supposed that the increasing rate acquired in both translational and rotational diffusion are not simply artifacts but can be the manifestation of some important phenomena like hot Brownian motion.
3. Though gold nanorod is bright enough to be resolved at a single particle level and has great potential to be integrated with TP-FCS as a rapid and ultrasensitive immunoassay in turbid media, an appropriate choice of the excitation power is closely related to the accuracy of the FCS measurement as they have very low saturation intensity. According to our results, tens of microwatts are the limitation for its usage. Even so, gold nanorod is still a superior TP-FCS probe than a fluorescent dye molecule as it provides greater brightness while eliminating possible photobleaching and photodamage effects, which is an important factor for an efficient, fast, and in situ measurement of a biological sample.

ACKNOWLEDGMENT

The authors acknowledge the integration of instruments by NSC that allowed them to perform the ICP-MS measurement at National Tsing Hua University, Taiwan. The two-photon fluorescence correlation spectroscopy was performed at the Center for Emerging Material and Advanced Devices, National Taiwan University.

REFERENCES

Agate B, Brown C, Sibbett W, Dholakia K. 2004. Femtosecond optical tweezers for in-situ control of two-photon fluorescence. Opt Express 12:3011–3017.

Bacia K, Schwille P. 2003. A dynamic view of cellular processes by in vivo fluorescence auto- and cross-correlation spectroscopy. Methods 29:74–85.
Barcellona ML, Gammon S, Hazlett T, Digman MA, Gratton E. 2004. Polarized fluorescence correlation spectroscopy of DNA-DAPI complexes. Microsc Res Tech 65:205–217.
Berland K, Shen G. 2003. Excitation saturation in two-photon fluorescence correlation spectroscopy. Appl Opt 42:5566–5576.
Berland KM, So PT, Gratton E. 1995. Two-photon fluorescence correlation spectroscopy: Method and application to the intracellular environment. Biophys J 68:694–701.
Bouhelier A, Bachelot R, Lerondel G, Kostcheev S, Royer P, Wiederrecht GP. 2005. Surface plasmon characteristics of tunable photoluminescence in single gold nanorods. Phys Rev Lett 95:267405.
Deng H-D, Li G-C, Dai Q-F, Ouyang M, Lan S, Gopal AV, Trofimov VA, Lysak TM. 2012. Role of interfering optical fields in the trapping and melting of gold nanorods and related clusters. Opt Express 20:10963–10970.
Ehrenberg M, Rigler R. 1974. Rotational brownian motion and fluorescence intensify fluctuations. Chem Phys 4:390–401.
Fu Y, Zhang J, Lakowicz JR. 2010. Plasmon-enhanced fluorescence from single fluorophores end-linked to gold nanorods. J Am Chem Soc 132:5540–5541.
Han Y, Alsayed AM, Nobili M, Zhang J, Lubensky TC, Yodh AG. 2006. Brownian motion of an ellipsoid. Science 314:626–630.
Huff TB, Tong L, Zhao Y, Hansen MN, Cheng J-X, Wei A. 2007. Hyperthermic effects of gold nanorods on tumor cells. Nanomedicine 2:125–132.
Jiang Y, Narushima T, Okamoto H. 2010. Nonlinear optical effects in trapping nanoparticles with femtosecond pulses. Nat Phys 6: 1005–1009.
Jones PH, Palmisano F, Bonaccorso F, Gucciardi PG, Calogero G, Ferrari AC, Marago´OM. 2009. Rotation detection in light-driven nanorotors. ACS Nano 3:3077–3084.
Larson DR, Zipfel WR, Williams RM, Clark SW, Bruchez MP, Wise FW, Webb WW. 2003. Water-soluble quantum dots for multiphoton fluorescence imaging in vivo. Science 300:1434–1436.
Link S, Burda C, Nikoobakht B, El-Sayed MA. 1999. How long does it take to melt a gold nanorod?: A femtosecond pump–probe absorption spectroscopic study. Chem Phys Lett 315:12–18.
Link S, Burda C, Nikoobakht B, El-Sayed MA. 2000a. Laser-induced shape changes of colloidal gold nanorods using femtosecond and nanosecond laser pulses. J Phys Chem B 104:6152–6163.
Link S, Wang ZL, El-Sayed MA. 2000b. How does a gold nanorod melt? J Phys Chem B 104:7867–7870.
Magde D, Elson E, Webb WW. 1972. Thermodynamic fluctuations in a reacting system—measurement by fluorescence correlation spectroscopy. Phys Rev Lett 29:705–708.
Malmqvist L, Hertz HM. 1995. Second-harmonic generation in optically trapped nonlinear particles with pulsed lasers. Appl Opt 34: 3392–3397.
Nagy A, Wu J, Berland KM. 2005. Observation volumes and γ-factors in two-photon fluorescence fluctuation spectroscopy. Biophys J 89: 2077–2090.
Pelton M, Liu M, Kim HY, Smith G, Guyot-Sionnest P, Scherer NF. 2006. Optical trapping and alignment of single gold nanorods by using plasmon resonances. Opt Lett 31:2075–2077.
Pitschke M, Prior R, Haupt M, Riesner D. 1998. Detection of single amyloid [beta]-protein aggregates in the cerebrospinal fluid of Alzheimer's patients by fluorescence correlation spectroscopy. Nat Med 4:832–834.
Rings D, Schachoff R, Selmke M, Cichos F, Kroy K. 2010. Hot brownian motion. Phys Rev Lett 105:090604.
Schwille P, Haustein E. 2009. Fluorescence correlation spectroscopy: An introduction to its concepts and applications. Spectroscopy 94: 1–33.
Sharma V, Park K, Srinivasarao M. 2009. Shape separation of gold nanorods using centrifugation. Proc Natl Acad Sci 106:4981–4985.
Thompson N. 1991. Fluorescence correlation spectroscopy, theory and applications. In: Lakowicz J, editor. Topics in fluorescence spectroscopy. New York: Plenum Press.
Tong L, Miljkovic VD, Käll M. 2009. Alignment, rotation, and spinning of single plasmonic nanoparticles and nanowires using polarization dependent optical forces. Nano Lett 10:268–273.
Toussaint KC, Liu M, Pelton M, Pesic J, Guffey MJ, Guyot-Sionnest P, Scherer NF. 2007. Plasmon resonance-based optical trapping of single and multiple Au nanoparticles. Opt Express 15: 12017–12029.
Tsay JM, Doose S, Weiss S. 2006. Rotational and translational diffusion of peptide-coated CdSe/CdS/ZnS nanorods studied by fluorescence correlation spectroscopy. J Am Chem Soc 128: 1639–1647.
Wang D-S, Hsu F-Y, Lin C-W. 2009. Surface plasmon effects on two photon luminescence of gold nanorods. Opt Express 17: 11350–11359.
Wang H, Huff TB, Zweifel DA, He W, Low PS, Wei A, Cheng J-X. 2005. In vitro and in vivo two-photon luminescence imaging of single gold nanorods. Proc Natl Acad Sci USA 102:15752–15756.
Widengren J, Rigler R. 1996. Mechanisms of photobleaching investigated by fluorescence correlation spectroscopy. Bioimaging 4: 149–157.
Wu J, Berland K. 2007. Fluorescence intensity is a poor predictor of saturation effects in two-photon microscopy: Artifacts in fluorescence correlation spectroscopy. Microsc Res Tech 70:682–686.
Zhang Y, Yu J, Birch DJ, Chen Y. 2010. Gold nanorods for fluorescence lifetime imaging in biology. J Biomed Opt 15:020504.